

## Electronic Supplementary Information (ESI)

### Interplay between surface chemistry and performance on rutile-type catalysts for halogen production

Maximilian Moser,<sup>a</sup> Vladimir Paunović,<sup>a</sup> Zhen Guo,<sup>a</sup> Laszlo Szentmiklósi,<sup>b</sup> Miguel G. Hevia,<sup>c</sup> Michael Higham,<sup>c</sup> Núria López,\*<sup>c</sup> Detre Teschner,\*<sup>d</sup> and Javier Pérez-Ramírez\*<sup>a</sup>

<sup>a</sup> Institute for Chemical and Bioengineering, Department of Chemistry and Applied Biosciences, ETH Zurich, Vladimir-Prelog-Weg 1, 8093 Zurich, Switzerland.

<sup>b</sup> Centre for Energy Research, Hungarian Academy of Sciences, Konkoly-Thege Miklós street 29-33, 1121 Budapest, Hungary.

<sup>c</sup> Institute of Chemical Research of Catalonia, ICIQ, Barcelona Institute of Science and Technology, BIST, Av. Països Catalans 16, 43007 Tarragona, Spain.

<sup>d</sup> Fritz-Haber-Institute of the Max Planck Society, Faradayweg 4-6, 14195 Berlin, Germany.

\*Corresponding authors. E-mails: [nlopez@iciq.es](mailto:nlopez@iciq.es) (N.L.)  
[teschner@fhi.mpg.de](mailto:teschner@fhi.mpg.de) (D.T.)  
[jpr@chem.ethz.ch](mailto:jpr@chem.ethz.ch) (J.P.-R.)

## Additional Computational Details

DFT calculations were performed over 33 different systems (besides the clean RuO<sub>2</sub>(110) surface) containing up to 6 Br atoms per *p*(2×1) surface unit cell of the RuO<sub>2</sub>(110) slab. For these calculations, the functional of choice was PBE-D2, thus including dispersion contributions. These may be relevant for the very polarisable Br atoms (S. Grimme, *J. Comp. Chem.*, 2006, **27**, 1787). Various configurations were tested for different relative positions of Br atoms (Fig. S3). For each configuration, the energy for the replacement of O atoms with Br was calculated using the reference reaction  $\text{RuO}_2 + 2n\text{HBr} \rightarrow \text{RuO}_2@\text{Br}_n + n\text{H}_2\text{O} + n/2\text{Br}_2$ , where *n* is the number of Br atoms incorporated. The most energetically favourable configurations were obtained for each Br incorporation. *Ab initio* thermodynamics were performed using these lowest energy configurations to determine the number of halogen atoms incorporated into the unit cell under typical experimental conditions as a function of the partial pressures *p*(HBr), *p*(H<sub>2</sub>O), and *p*(Br<sub>2</sub>) (Figs. 2, S6, and S7). An analogous procedure was followed to determine the extent of Cl uptake of RuO<sub>2</sub>(110) and the outcome is presented in the same figures.

Similar calculations were also performed to investigate the Br uptake of TiO<sub>2</sub>(110). However, they are less exhaustive since the extent of bromination of titanium oxide is much lower compared than that of ruthenium oxide. Thus, DFT calculations were performed for 4 distinct configurations investigating the incorporation of up to 2 Br atoms into a *p*(2×2) cell at 6-coordinate bridging sites in comparison to the clean slab (Fig. S8). As for RuO<sub>2</sub> halogenation, the structures were relaxed and replacement energies calculated. The lowest energy configurations were used in *ab initio* thermodynamics studies of the surface composition as a function of *p*(HBr) and *p*(H<sub>2</sub>O) (Figs. 2 and S6).

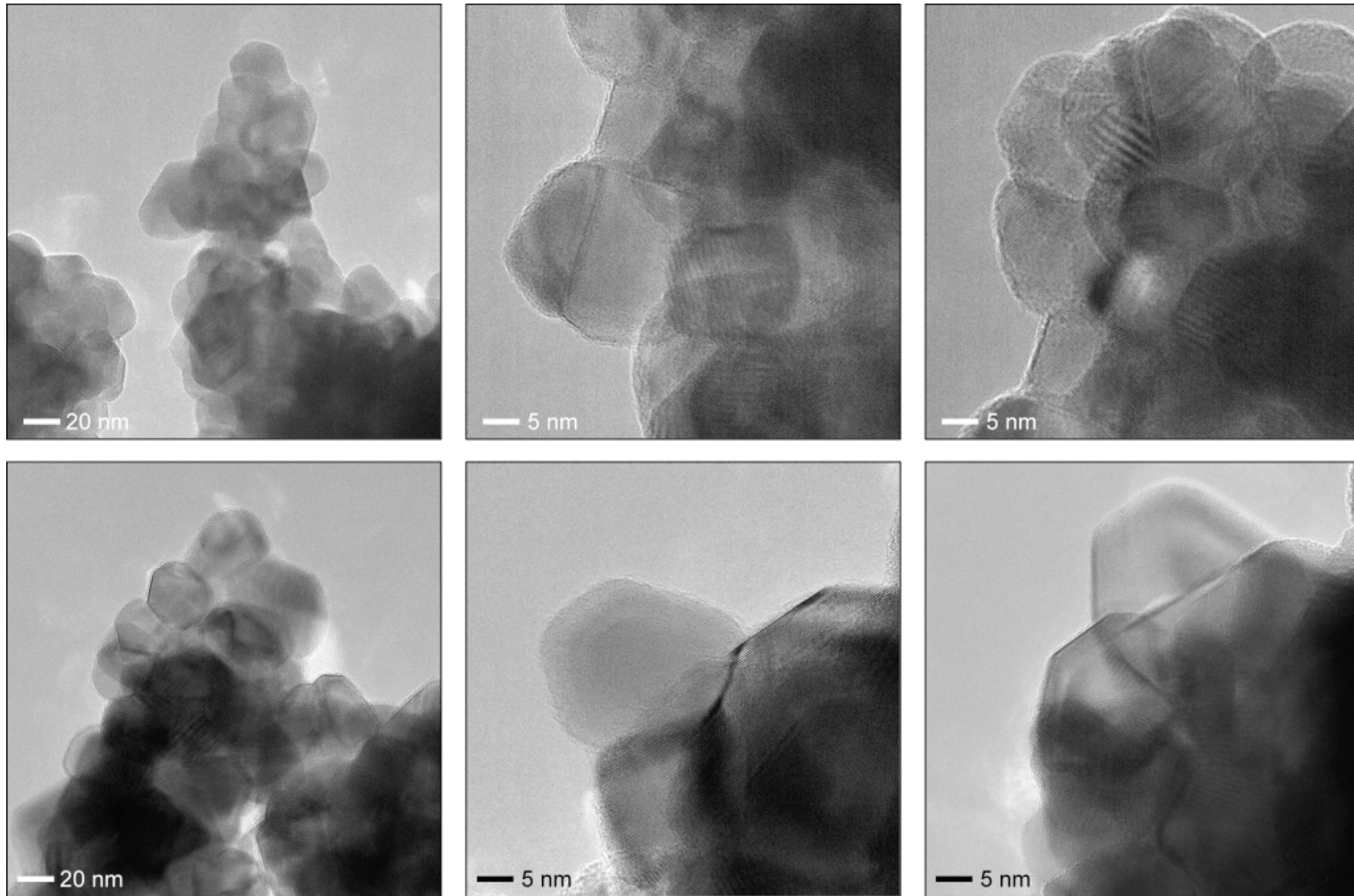


**Fig. S1.** HRTEM of RuO<sub>2</sub> treated in HBr at 393 K (top micrographs) and HCl at 543 K (bottom micrographs) for 3 h.

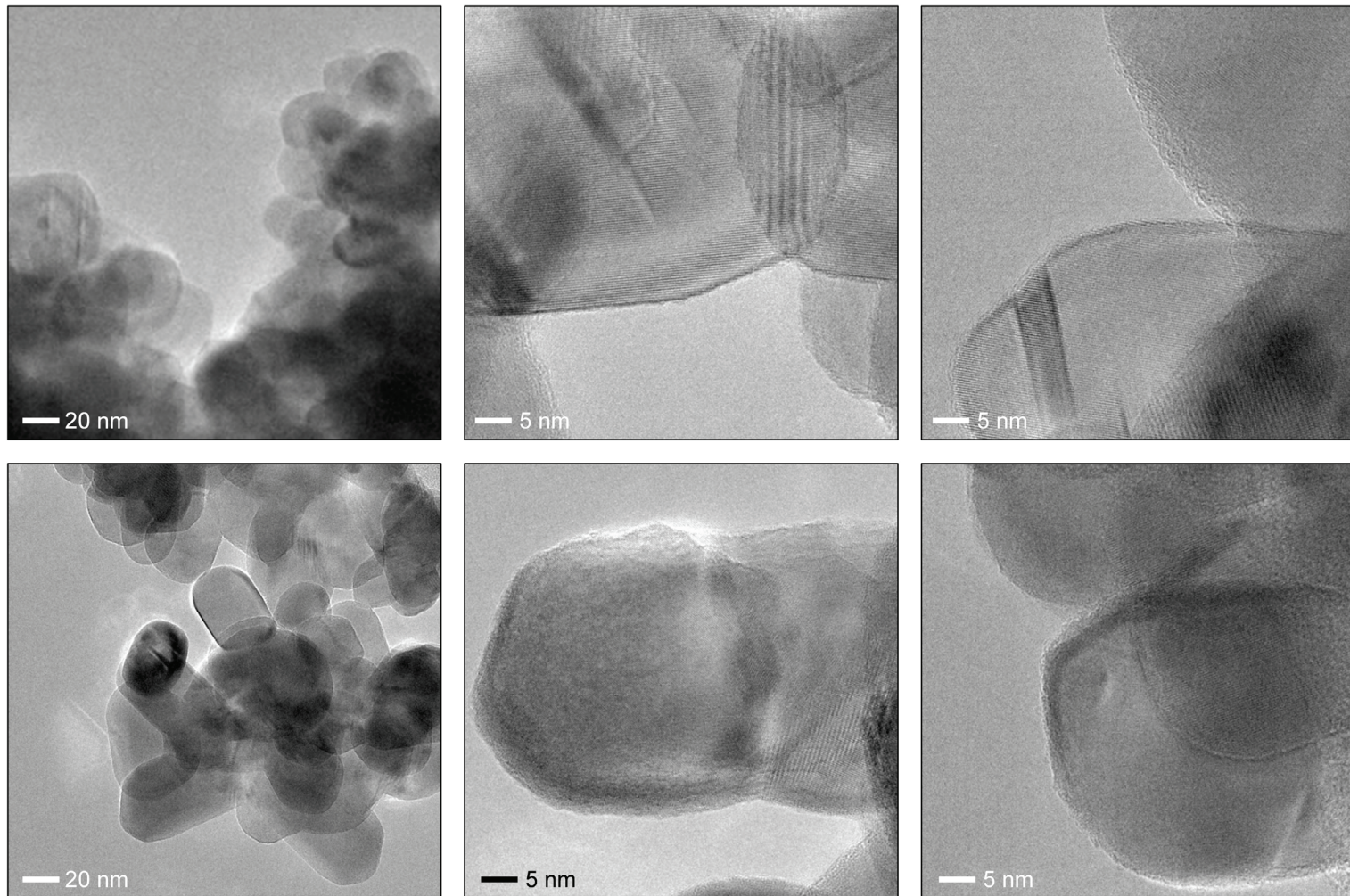


**Fig. S2.** HRTEM of  $\text{TiO}_2$  treated in HBr at 573 K (top micrographs) and HCl at 633 K (bottom micrographs) for 3 h.

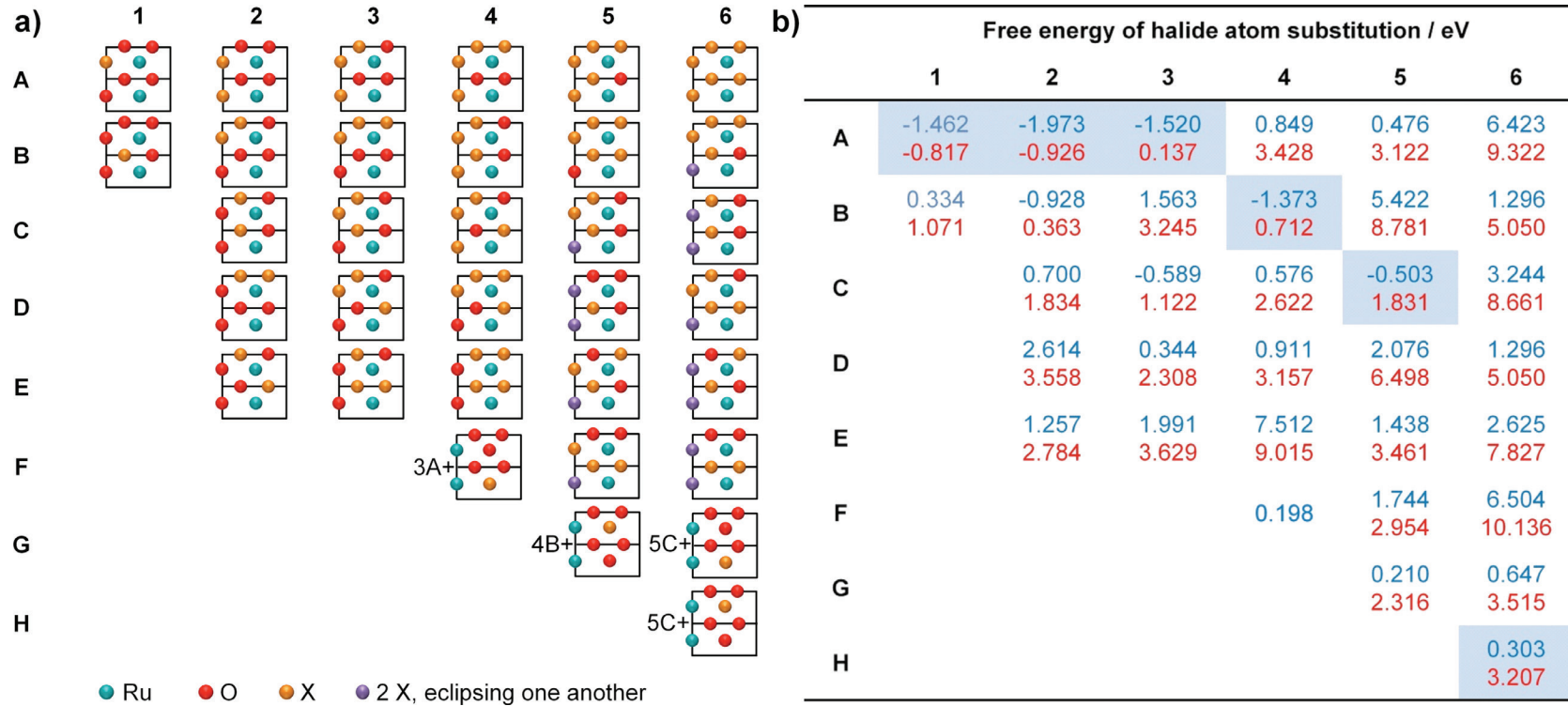


**Fig. S3.** Schemes of the incorporation of halogen atoms ( $X = \text{Br}, \text{Cl}$ ) into a  $(2 \times 1)$  cell for the  $\text{RuO}_2(110)$  surface (a). The number of substituted halide atoms (1-6) as well as their relative position in the lattice (A-H) was computed for 33 different configurations. Configurations 4F, 5G, 6G, and 6H depict the halogen substitution into the subsurface layer, whereby the surface configurations are identical to 3A, 4B, and 5C, as indicated in (a). The free energy values of Br (blue values) and Cl (red values) atom substitution for all configurations are listed in (b). Blue boxes indicate the lowest free energy cases.

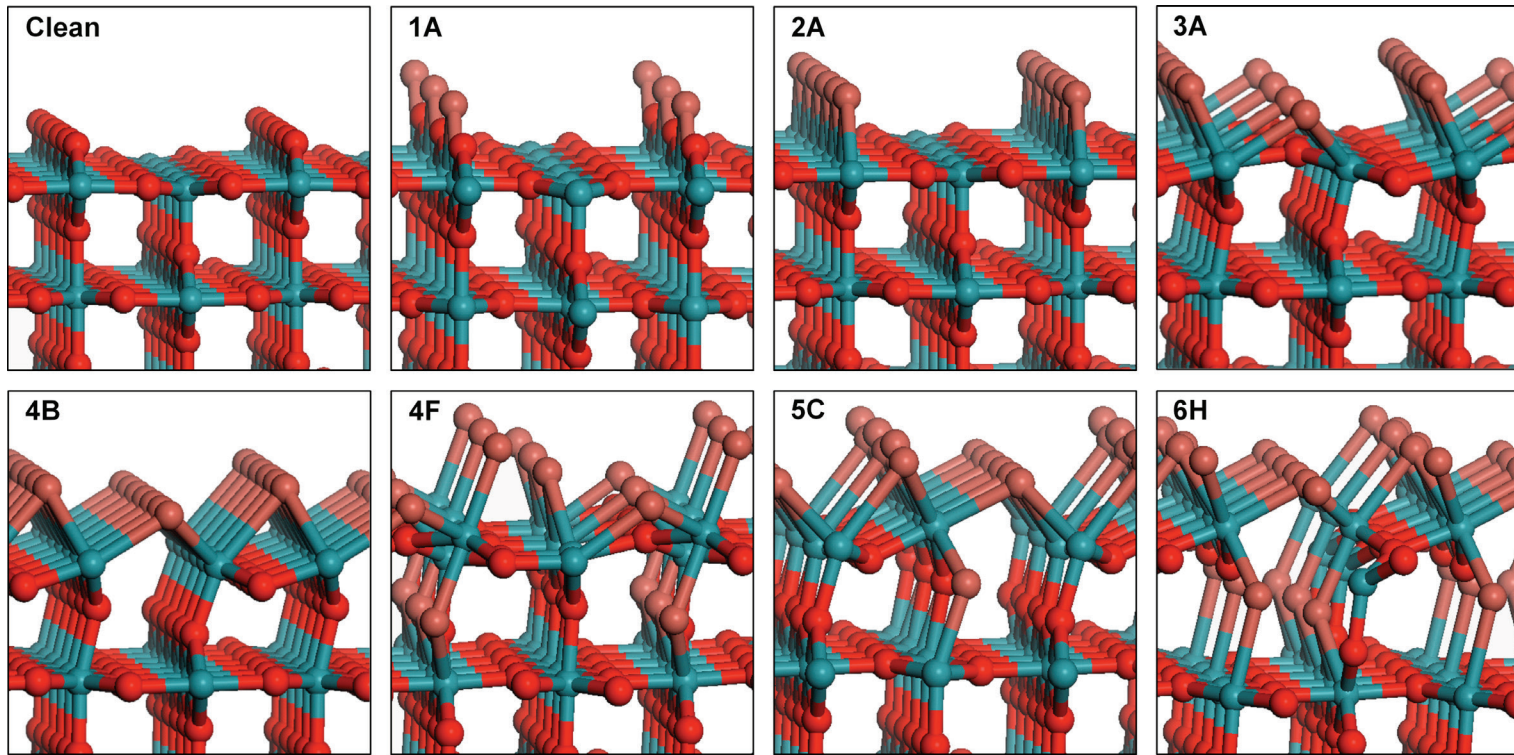


**Fig. S4.** Clean and Br substituted RuO<sub>2</sub> surfaces having the lowest free energies as listed in Figs. 2 and S3b. Colour code: Ru (blue), O (red), and Br (brown). Notice the distorted rutile structure upon a certain degree of bromination.

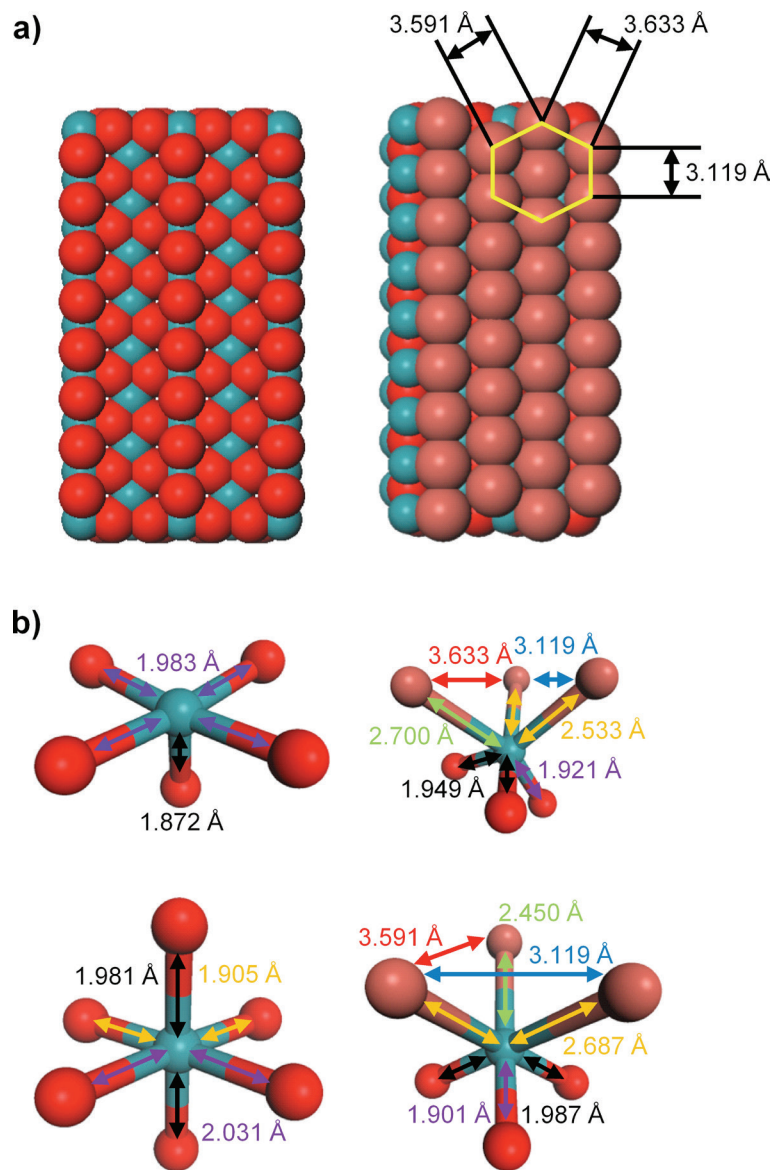


**Fig. S5.** Regular  $\text{RuO}_2(110)$  slab (left) and 4B configuration (right) are presented for comparison depicting the distinctive hexagonal arrangement of bromine atoms on the surface (a). Local surface coordination environments of the  $\text{Ru}_{\text{cus}}$  site (top) and 6-coordinate Ru site (bottom) for the regular slab (left) and for the 4B configuration (right) are shown in (b). Colour code: Ru (blue), O (red), and Br (brown).

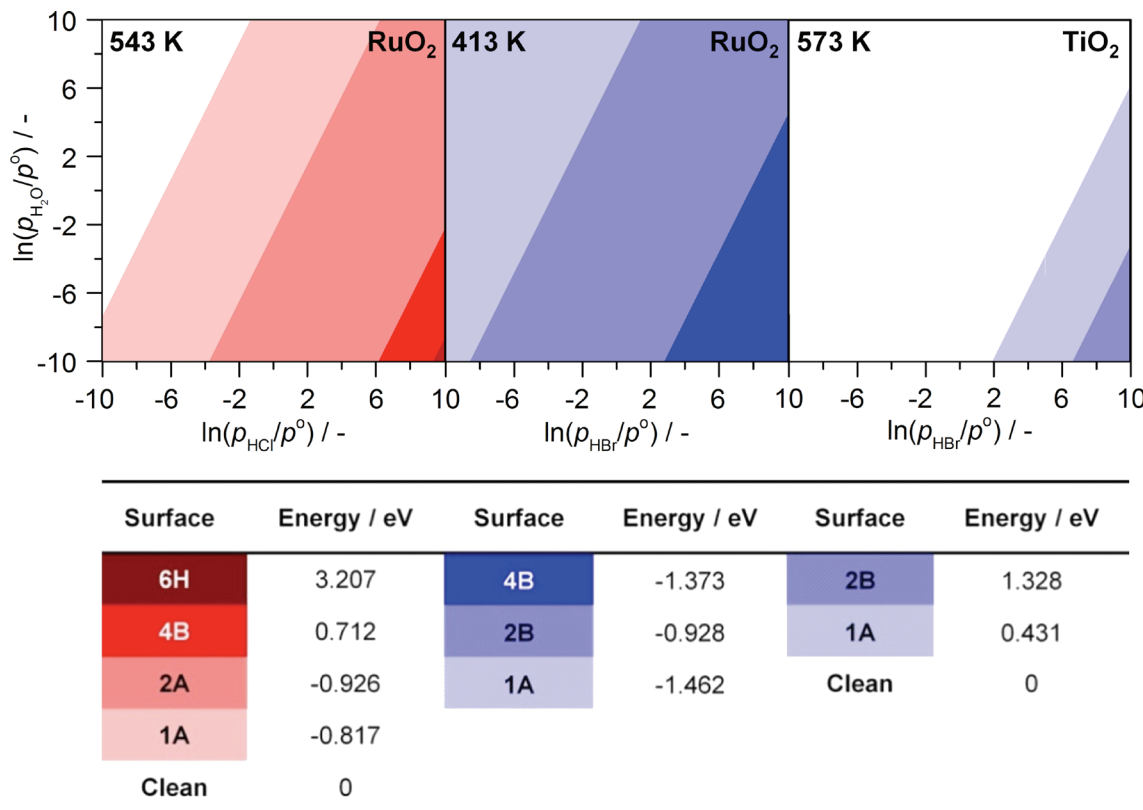


**Fig. S6.** *Ab initio* thermodynamics of the Cl (red) and Br (blue) substitution on MO<sub>2</sub>(110) surfaces. The colour shades denote the surface configurations in Figs. S3 and S8 having the lowest energies under the simulated conditions. The partial pressures of Cl<sub>2</sub> and Br<sub>2</sub> were fixed at 1 bar.

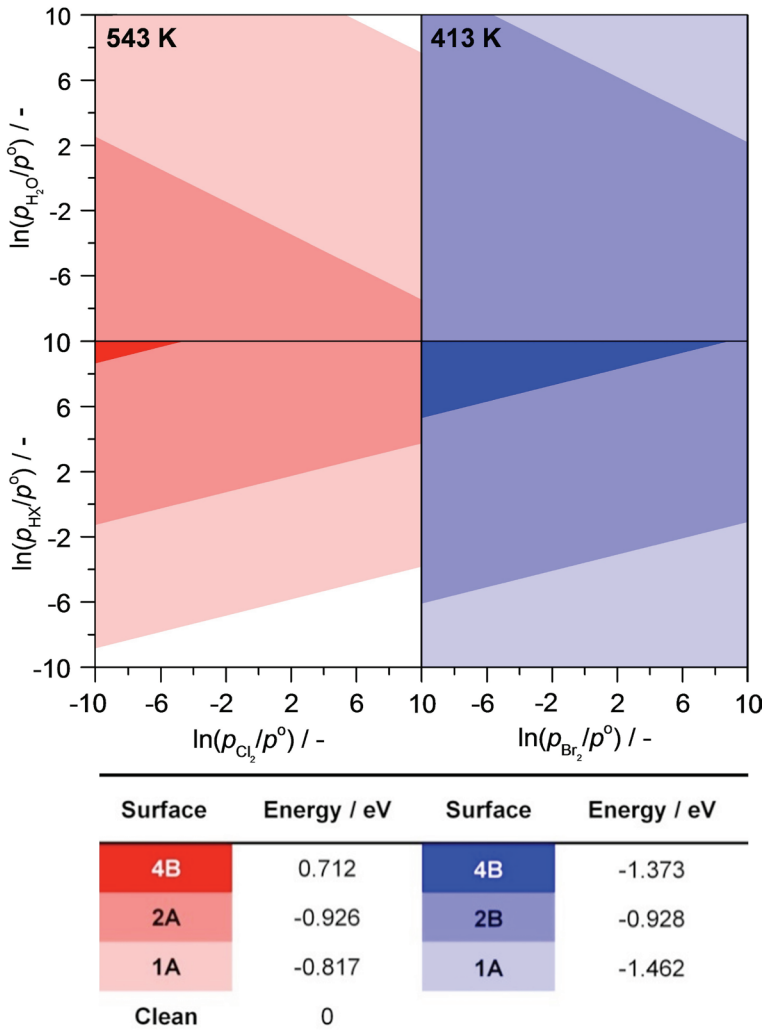


**Fig. S7.** *Ab initio* thermodynamics of the Cl (red) and Br (blue) substitution on RuO<sub>2</sub>(110) surfaces. The colour shades correspond to the surface configurations in Fig. S3 having the lowest energy under the simulated conditions. The partial pressures of HX (top) and H<sub>2</sub>O (bottom) were fixed at 1 bar.

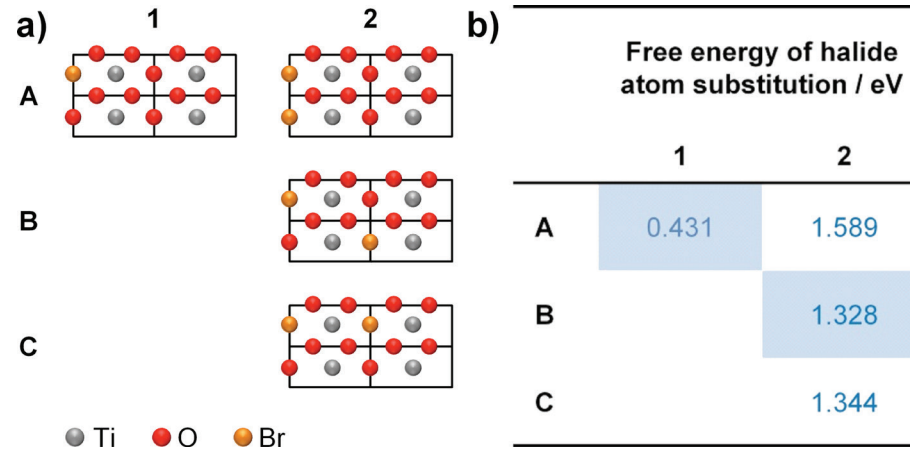


**Fig. S8.** Schemes of the incorporation of bromine atoms into a (2×2) cell for the  $\text{TiO}_2(110)$  surface (a). The number of substituted halide atoms (1-2) as well as their relative position in the lattice (A-C) was computed for 4 different configurations. The free energy values of Br substitution for all configurations are listed in (b). Blue boxes indicate the lowest free energy cases.

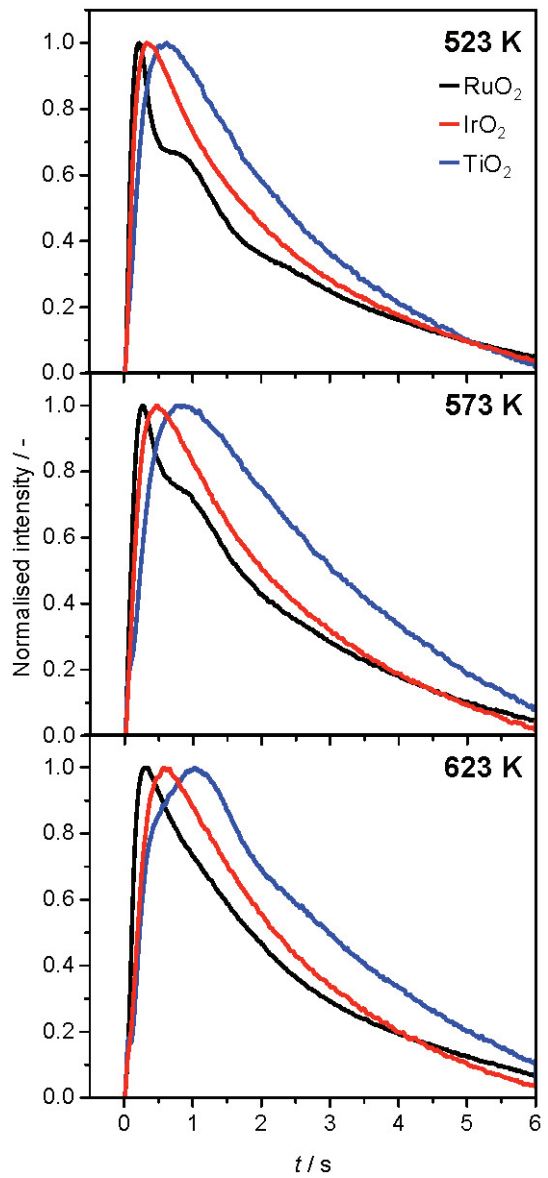


**Fig. S9.** Normalised transient responses of HBr upon individual pulsing of HBr over rutile-type catalysts at different temperatures.

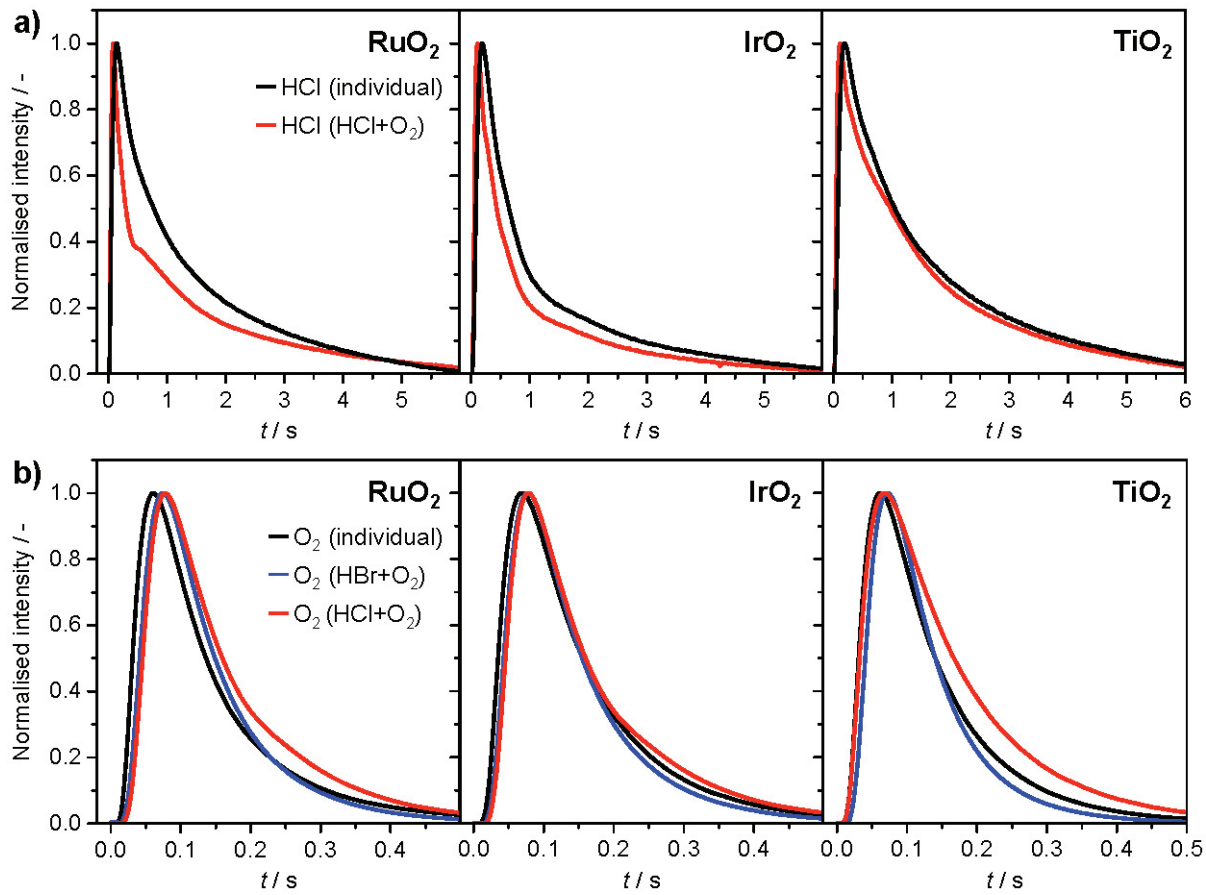


**Fig. S10.** Normalised transient responses of HCl at 623 K upon HCl (black) and HCl+O<sub>2</sub> (red) pulsing (a). Normalised transient responses of O<sub>2</sub> at 623 K upon O<sub>2</sub> (black), HBr+O<sub>2</sub> (blue), and HCl+O<sub>2</sub> (red) pulsing (b).

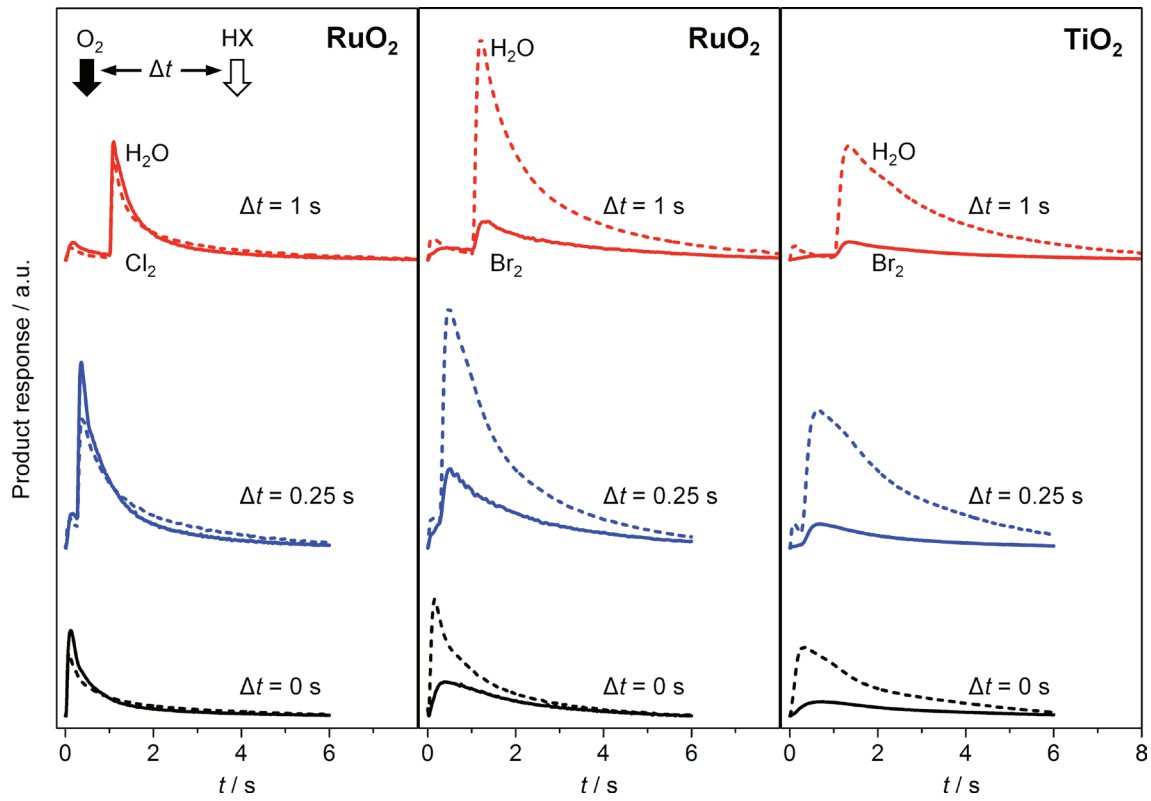


**Fig. S11.** Transient responses of  $\text{Br}_2$  and  $\text{Cl}_2$  (solid lines) as well as  $\text{H}_2\text{O}$  (dashed line) in pump-probe experiments with  $\text{O}_2\text{-HBr}$  and  $\text{O}_2\text{-HCl}$  at variable time delay ( $\Delta t$ ) over  $\text{RuO}_2$  and  $\text{TiO}_2$  at 623 K. The order of the pump and probe molecules is depicted in the top-left corner.

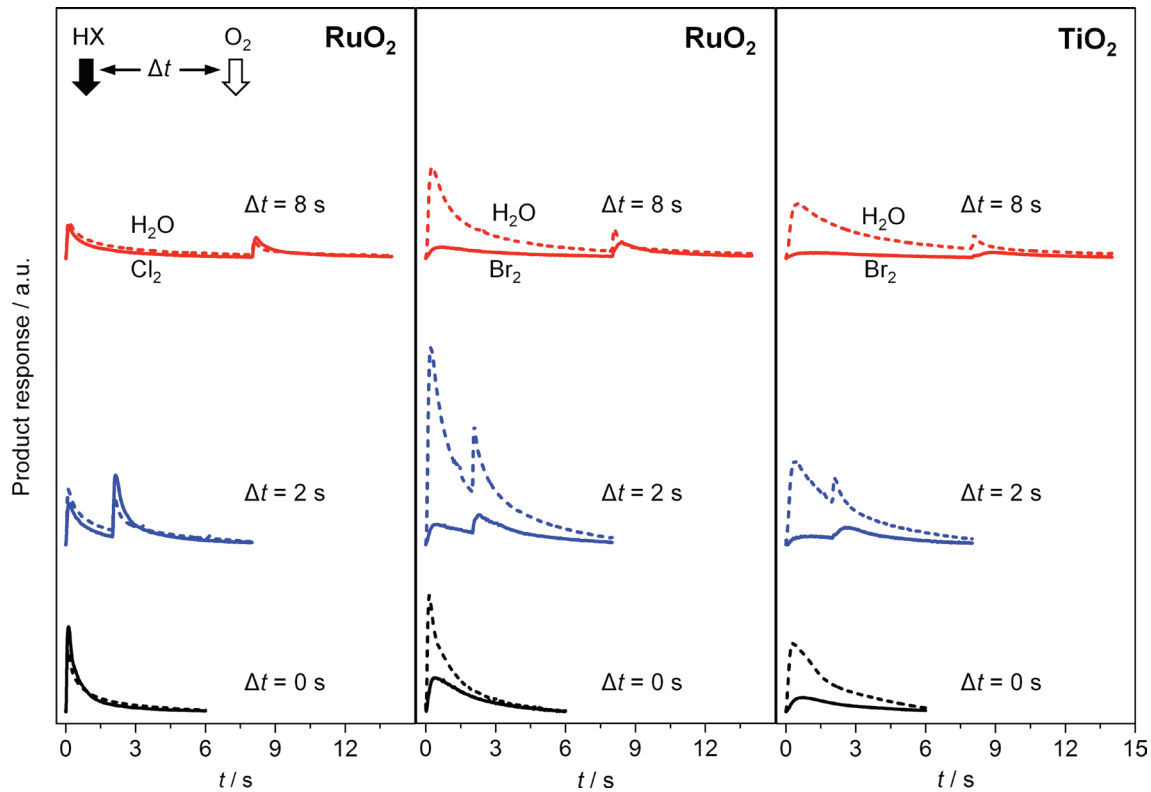


**Fig. S12.** Transient responses of  $\text{Br}_2$  and  $\text{Cl}_2$  (solid lines) as well as  $\text{H}_2\text{O}$  (dashed line) in pump-probe experiments with  $\text{HBr-O}_2$  and  $\text{HCl-O}_2$  at variable time delay ( $\Delta t$ ) over  $\text{RuO}_2$  and  $\text{TiO}_2$  at 623 K. The order of the pump and probe molecules is depicted in the top-left corner.

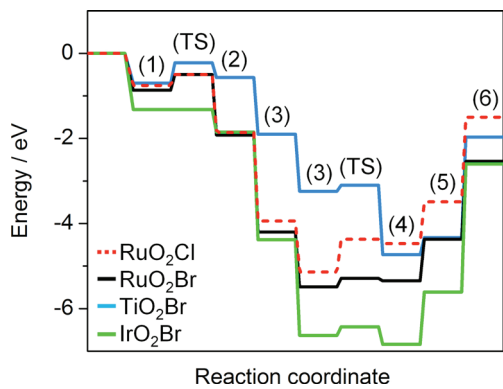


**Fig. S13.** Reaction profiles of HBr (solid lines) and HCl (dashed line) oxidation on halogenated rutile-type catalysts. Herein, (1) is the molecular O<sub>2</sub> adsorption and (2) is the dissociated state after the transition state (TS). Subsequently, two HX molecules are adsorbed in steps (3), followed by the transition state (TS) for the OH recombination to water (4). Finally, both water (5) and molecular halogen (6) are desorbed from the surfaces. The profile corresponds to half a stoichiometric reaction: O<sub>2</sub> + 2HX → O\* + H<sub>2</sub>O + X<sub>2</sub>, thus step (3) occurs only twice and an oxygen atom is left on the surface in the final state.

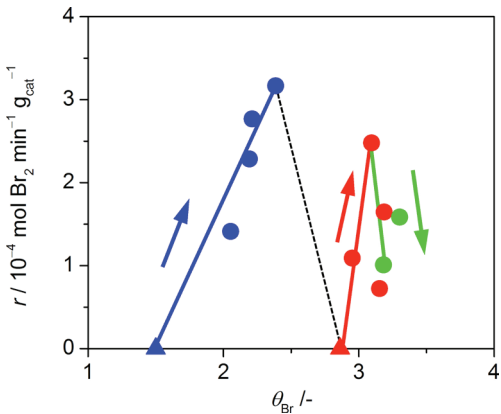


**Fig. S14.** Rate of bromine formation versus bromine coverage on RuO<sub>2</sub>. After pre-treatment at O<sub>2</sub>:HBr = 0 and 393 K (blue triangle), the temperature was gradually increased from 393 K to 433 K in steps of 10 K (blue circles). Afterwards, the pre-treatment was repeated (red triangle) before increasing the O<sub>2</sub>:HBr ratio in the order 1, 2, 4, and 9 at 413 K (red circles). Finally, the O<sub>2</sub>:HBr ratio was decreased from 9 to 4 and 2 at 413 K (green circles). Despite the increase in temperature and O<sub>2</sub> content of the feed mixture, RuO<sub>2</sub> gradually increases its bromine uptake, which exceeds the maximal theoretical coverage by up to 3 times and thus indicates subsurface bromination of RuO<sub>2</sub>.

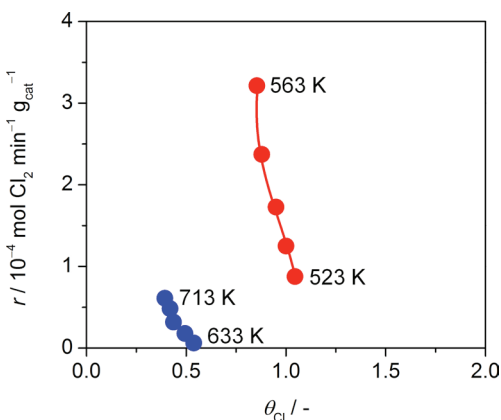


**Fig. S15.** Rate of chlorine formation versus chlorine coverage over TiO<sub>2</sub> (blue circles) and RuO<sub>2</sub> (red circles) at O<sub>2</sub>:HCl = 2 and different temperatures. The temperature was increased from 633 K to 713 K in steps of 20 K for TiO<sub>2</sub>, and from 523 K to 563 K in steps of 10 K for RuO<sub>2</sub>.